Universiteit Utrecht

Koninklijk Nederlands
Meteorologisch Instituut
*Ministerie van Infrastructuur en Waterstaat*

# Climate Dependence of Arctic Precipitation Variability


Linda Bogerd

June 2019

*Supervisors:*

| | |
|---|---|
| Richard Bintanja | (KNMI, RUG) |
| Eveline C. van der Linden | (KMNI, WUR) |
| Folmer Krikken | (KNMI) |
| Michiel R. van den Broeke | (UU) |

# Abstract

The increase in Arctic precipitation is expected to amplify more rapidly than the global mean in warming climates. However, the warming-induced changes in variability of Arctic precipitation, evaporation, and poleward moisture transport are currently largely unknown. This study compares the precipitation variability in quasi-equilibrium climates with different $CO_2$ concentrations from a global climate model and studies the underlying mechanisms. Five quasi-equilibrium simulations of 400 years forced with a broad range of $CO_2$ concentrations (0.25, 0.5, 1, 2, and 4 times the current global mean) using the EC-Earth model were analyzed. Poleward moisture transport variability is presumably responsible for Arctic precipitation variability in colder climates as the ocean in the Arctic basin is completely covered by sea ice. Arctic precipitation variability increases towards warmer climates primarily in summer, because of i) the strong increase in mean precipitation in winter due to enhanced evaporation (which exerts a comparatively small increase in variability), ii) the strong interaction between poleward moisture transport and evaporation in winter, and iii) the increasing relation between Arctic sea level pressure variability and precipitation variability in summer in warmer climates.

# 1. Introduction

Global warming will affect the Earth's hydrological cycle because the moisture holding capacity of the atmosphere is increased. Such changes can severely affect the living environment of people and animals, for instance because the risk of floods is increased due to more frequent and intense rainfall (Hassol, 2006; IPCC, 2013). A proper understanding of the changes in the hydrological cycle in a warmer climate is therefore crucial for assessing future climate impacts.

While climate warming will affect precipitation rates over the entire globe, the increases in the Arctic region are projected to be particularly severe. The comparatively strong increase in Arctic precipitation is caused by two main climate mechanisms. First, because the Arctic warms faster than other parts of the world (known as Arctic amplification) (Manabe and Stouffer 1980; Serreze and Francis 2006), the Arctic atmosphere can hold more moisture. Second, the increase in precipitation per degree of warming is relatively large at 4.5% per K in the Arctic region (globally this increase is ~2% per K (Held & Soden, 2006)). This increase can be attributed mainly to sea ice retreat, causing strongly enhanced surface evaporation (Bintanja & Selten, 2014).

Freshening of the Arctic ocean, due to increased Arctic precipitation, ice melting, and enhanced continental run-off might affect the Atlantic Meridional Overturning Circulation (AMOC) (Bintanja & Selten, 2014), which in turn can modulate the climate in Europe (Meier et al., 2012). Also, the increase in atmospheric moisture amplifies polar warming by strengthening the water vapor and cloud feedbacks (Eastman & Warren, 2010; Vavrus & Harrison, 2003). Hence, it is of importance to study this region in more depth, as changes in the Arctic's hydrological cycle may have local and wide-ranging effects.

Most research on the hydrological cycle has focused on assessing trends in mean quantities. However, since strong variations can persist on interannual and decadal timescales, especially in the Arctic, climate variability can temporarily obscure or enhance trends (Hawkins & Sutton, 2009; Screen et al., 2014). Increased knowledge about the frequency and magnitude of the variability, as well as the processes behind climate variability, can help interpret climate trends. Moreover, the

interannual variability of the hydrological cycle is one of the governing aspects of precipitation extremes (Pendergrass et al., 2017).

Internal climate variability in the Arctic is associated mainly with the large-scale atmospheric circulation and pressure systems. In the Arctic region, the Arctic Oscillation is the most significant mode of variability, which is found to be strongly linked to precipitation variability (Boer et al., 2001; Groves & Francis, 2002; Oshima & Yamazaki, 2004). It has been shown that the relation between atmospheric circulation and temperature variability changes towards warmer climates, because of the diminishing role of sea ice due to melting (van der Linden et al., 2017, Reussen et al., *under review*).

Variability in the meridional moisture gradient can also alter the Arctic's hydrological variability by affecting the poleward moisture transport. In warmer conditions, sea ice variability will decrease (Reussen et al., *under review*), which is expected to influence the variability in the amount of atmospheric moisture in the Arctic through evaporation. How these changes will affect precipitation variability is, however, not yet understood.

This study will identify climate mechanisms that govern the variability of the Arctic's hydrological cycle (with the main focus on precipitation variability) by evaluating model-simulated climate response to changed concentrations of $CO_2$. Four long climate simulations representing colder and warmer than present quasi-equilibrium climates will be used to elucidate differences in climate variability between climate states. Special attention is given to the mechanisms that drive changes in poleward moisture transport variability (separating the thermodynamic and dynamic contributions). Eventually, our results will show what processes dominate the changes in the hydrological cycle, including those in variability, which helps to quantify and interpret future changes in climate extremes in the Arctic, as well as their potential impacts.

# 2. Methods

## 2.1. Model and Simulations

*Global Climate Model*

Datasets of long duration (e.g. centuries) are the most appropriate to study (decadal) climate variability. Both reanalyses and observations are, unfortunately, not available over such long time periods. Moreover, observations over the Arctic are sparse, are usually associated with high uncertainties (especially precipitation), and commonly exhibit long-term forced trends. Therefore, we will use a state-of-the-art fully coupled global climate model (GCM) in long quasi-equilibrium simulations to assess climate variability. It concerns the EC-Earth model, version 2.3 (Hazeleger et al., 2012), which was used in the Coupled Model Intercomparison Project phase 5 (CMIP5) for the most recent IPCC report (Taylor et al., 2012).

The atmospheric, oceanic, and land surface components are coupled by the Ocean, Atmosphere, Sea Ice, Soil (OASIS) coupling module (Valcke et al., 2003). The Integrated Forecast System (IFS) of the European Center for Medium-range Weather Forecasts (ECMWF) for the atmospheric component runs at T159 spectral resolution with a vertical resolution of 62 height levels. The Nucleus for European Modelling of the Ocean (NEMO) model for the ocean uses a horizontal grid configuration with a resolution of approximately 1.1 degrees and a vertical resolution of 42 levels. The performance of the EC-Earth model in the Arctic in terms of the mean and variability (e.g. Arctic Oscillation) can be found in Koenigk et al. (2013) and Reussen et al. (*under review*), respectively. The EC-Earth model is capable of simulating atmospheric dynamics (Reussen et al., *under review*) and realistic evaporation values (Koenigk et al., 2013).

Equilibrium climates are appropriate to analyze climate variability because there is no forced component that influences the variability. Therefore, five simulations with fixed $CO_2$ concentrations (multiplications of 0.25, 0.5, 1, 2, and 4 compared to the present-day $CO_2$ concentration, van der Linden et al., 2017) were studied. First, the initial state of the control climate was obtained from a spin-up of pre-industrial forcing over about 1000 years, after which

integration with present-day variables (e.g. emission concentrations, land use, and forcing in the year 2000) was carried out over 44 years. Constant $CO_2$ fractions were then set, after which the integrations continued for another 550 years for each $CO_2$ value (van der Linden et al., 2019). The ocean surface was assumed to be in equilibrium after 150 years (Reussen et al., *under review*; van der Linden et al. 2017), hence only the last 400 years of the simulations were studied.

*Validation with reanalyses data*

To validate the performance of the EC-earth model in the Arctic, the control simulation was compared to reanalyses data (NASA MERRA-2 (Gelaro et al., 2017), ERA-Interim (Dee et al., 2011), and NCEP / CSFR (Saha et al., 2010)). Because of the large observational uncertainties over the Arctic area, and the relatively short time period (especially for interannual variability), a multi-reanalyses mean is expected to be the most accurate for model validation. Hence, we took the average of the three reanalyses datasets (both in the mean and in variability) and compared the values from 1980-2010 (as being representative for the present-day climate) with those from the EC-Earth control simulation.

**2.2. Components in the Arctic moisture budget**

The following monthly variables were extracted from the model for analysis: total precipitation (TP) (defined as convective precipitation + large-scale precipitation), specific humidity, surface evaporation (E), sea level pressure, geopotential height, sea surface temperature, and sea ice concentration. Other climate variables of importance were calculated as specified below.

*Total precipitable water*

Specific humidity [kg/kg] (q) was converted and integrated over height to total precipitable water [mm] (Q). The integration was performed from 1000 hPa to 20 hPa over 16 height intervals (the moisture concentration was negligible above 20 hPa). The integration was performed with the trapezoidal method (following Dufour et al. 2016):

$$Q = \frac{-1}{g}\int_{surface}^{top} qdp = \frac{\sum_{surface}^{top} q_n + q_{n+1}{}^{*}(p_n - p_{n+1})}{2^{*}g}$$

with $g$ the gravitational acceleration and $p$ the pressure level.

*Moisture transport into the Arctic (moisture convergence)*

Meridional moisture transport is usually calculated by evaluating $\nabla qv$ over a latitude circle. However, over sufficiently long-time intervals (e.g. seasonal and annual), the balance method is much easier to apply and quite accurate (Bengtsson et al., 2011), especially when the storage term is included (Dufour et al., 2016). Hence, the moisture transport into the Arctic (70 °N - 90 °N) through 70 °N was determined from the following relation (Dufour et al., 2016; Groves & Francis, 2002):

$$-\nabla qv = TP - E + \frac{\partial Q}{\partial t}$$

where the ∂Q/dt-term was calculated using central differences. Despite the small moisture holding capacity in the Arctic, the ∂Q/∂t-term (the tendency of precipitable water) is not negligible (Oshima & Yamazaki, 2004; Sorteberg & Walsh, 2008), especially during spring and fall seasons. As temperature increases, this term is expected to become more important due to the associated increase in atmospheric moisture holding capacity (i.e. the atmosphere can retain more water until it is saturated and precipitates out). This is due to the exponential relation (known as the Clausius Clapeyron relation) between specific humidity and temperature.

*Geostrophic wind at 500 hPa*

The geopotential height ($\Phi$) at 500 hPa is often used as a proxy for storm tracks (Meehl et al., 2001; Pinto et al., 2007). From the geopotential height the geostrophic wind speed ($\vec{v}_g$) can be calculated, which has the advantage of including the geopotential gradient. Therefore, temperature changes across the climate states are filtered out. This variable was calculated by using the following relations:

$$u = \frac{-g}{f^{*}r}\frac{\partial \Phi}{\partial \varphi}$$

$$v = \frac{g}{f * r * \cos(\varphi)}\frac{\partial \Phi}{\partial \lambda}$$

$$\vec{v}_g = \sqrt{u^2 + v^2}$$

where $u$ and $v$ are, respectively, the zonal and meridional wind components, $f$ the Coriolis parameter (defined as $f = 2\ \Omega \sin \varphi$ with $\Omega$ ($7.2921 \times 10^{-5}$ rad $s^{-1}$) the rotation of the Earth), $\lambda$ the longitude, $\varphi$ the latitude, and $r$ the radius of the Earth.

*Arctic Oscillation*

Multiple studies have shown the relation between the Arctic Oscillation (AO) and the meridional moisture transport (Groves & Francis, 2002; Oshima & Yamazaki, 2004; Jakobson & Vihma, 2010). Therefore, it is vital to analyze the AO-index, in particular because the AO-index may become more positive in warmer climates (Gillett, 2002; Rind et al., 2005). The AO-index is linked to the dominant sea level pressure pattern associated with variability for 20 °N - 90 °N (Thompson & Wallace, 1998) and was calculated as the strength of the first principle component of the empirical orthogonal function (EOF) in sea level pressure. The effect of the AO is more pronounced in winter (Boer et al., 2001; Jakobson & Vihma, 2010), but in summer the impact of the AO is potentially more important due to the abundance of atmospheric moisture (Groves & Francis, 2002).

**2.3. Analyses**

*Interannual and decadal*

Oceanic transport is a relatively slow process compared to the atmospheric moisture transport because of the relatively small heat capacity of the atmosphere. It is therefore expected that temporal variability on shorter time scales (interannual) are potentially linked to other mechanisms than for longer-term (decadal) variabilities (as already is found to be the case for temperature as studied by Reussen et al., *under review*). To assess such differences, the time series were subdivided into high and low frequencies. After the annual and seasonal averages were calculated, and the averaged data were linearly detrended, a fourth-order Butterworth filter with a cut-off frequency of 0.1 $yr^{-1}$ was applied. Henceforth we refer to interannual variability (periodicity shorter than 10 years) and decadal variability (larger than 10 years).

*Seasonal patterns*

The present-day Arctic climate is characterized by distinct seasonal patterns in the hydrological cycle. In winter, the variability in the number and intensity of cyclones infiltrating the Arctic region is comparatively high (Sorteberg & Walsh, 2008), associated with amplified poleward moisture transport. Furthermore, strong evaporation occurs over the North Atlantic (Jakobson & Vihma, 2010), and the AO is most pronounced (Groves & Francis, 2002; Thompson & Wallace, 1998). In summer, the moisture content in the air is highest (Groves & Francis, 2002; Jakobson & Vihma, 2010) and the absolute magnitude of precipitation variability is found to be the largest (as discussed in section 3.2). Because of these seasonal dependencies in variables and (presumably) the mechanisms behind Arctic climate variability, we will focus mainly on the winter (DJF) and summer (JJA) patterns and the differences between these patterns.

*Variability*

The standard deviation was used as a metric for the variability because this is a frequently used metric for precipitation variability (Pendergrass et al., 2017; Boer, 2009; Groves & Francis, 2002). The Arctic region was chosen to cover the area 70 °N – 90 °N (Groves & Francis, 2002; Oshima & Yamazaki, 2004; Sorteberg & Walsh, 2008). Relations between variables were examined by calculating their regressions and correlations. The spatial patterns of precipitation variability were quantified with EOF analysis.

In order to give an indication of the uncertainty in the means and standard deviations, a bootstrap test (with 1000 random samples) was performed on the seasonal averaged and detrended data. In this method, random data points are taken from the original dataset (with replacement) of which a new sample (of the same size, in our case 400 data points) is created. The associated 5 and 95 percentiles are used to indicate the error bars. The same method is used to mark significant differences between the reanalyses and simulated variability. Differences are marked as significant if the $95^{th}$ percentile of the reanalyses (simulation) is smaller than the $5^{th}$ percentile of the simulation (reanalyses).

# 3. Results

## 3.1. Characteristics of the Arctic and model validation

*Mean precipitation*

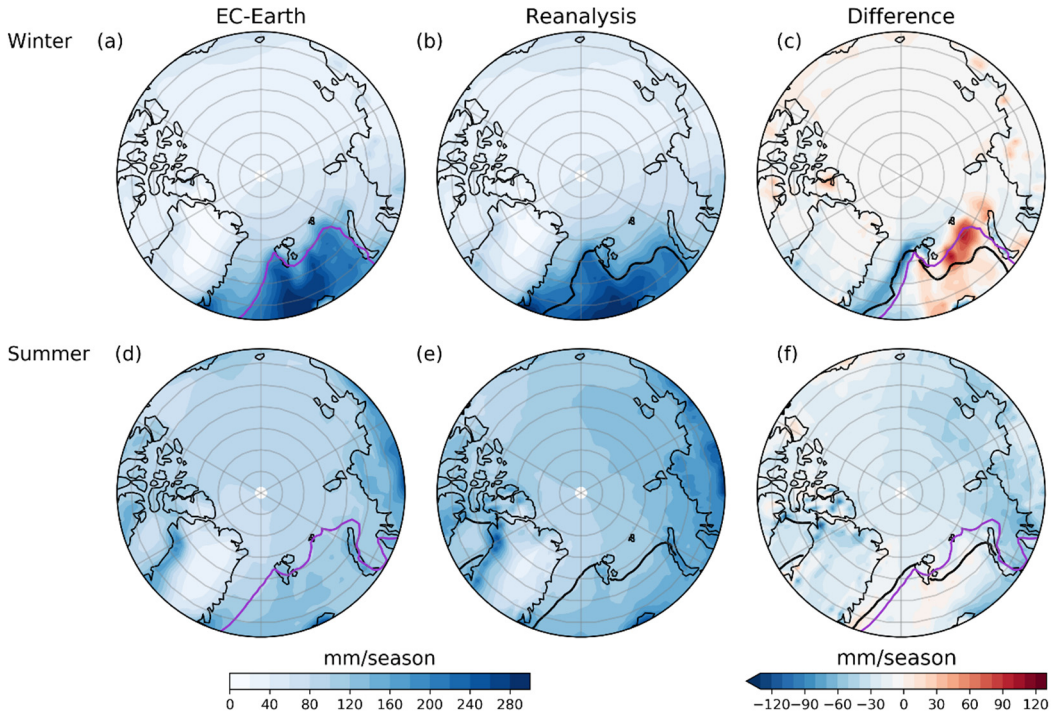


**Figure 1**: Mean precipitation for EC-Earth (the control simulation), reanalyses (defined as the average value for ERA-Interim, NCEP/CSFR, and NASA MERRA-2), and the difference (reanalyses - EC-Earth) for winter (first row) and summer (second row). The purple and black contours indicate the 15% sea ice concentration isopleth.

The precipitation means in both winter and summer for the EC-Earth control climate and the reanalyses are shown in Fig. 1, together with the respective differences. The contours indicate the 15% sea ice concentration isopleth, which is an often-used definition of the sea ice edge (Deser et al., 2000; Zhang et al., 2013). For both winter and summer, high precipitation rates are observed near the margins of Greenland because of orographic uplifts caused by the high elevation of the

ice sheet. As air is forced to rise, it cools adiabatically, resulting in condensation and precipitation. The precipitation decreases with increasing latitude and altitude because of colder air temperatures, which limits the moisture holding capacity of the atmosphere.

In winter, the highest precipitation rates are over the North Atlantic Ocean (Fig. 1a and 1b). This is due to: i) the vertical instabilities caused by the relativity warm open water but cold air temperature (Serreze and Hurst 2000), which causes high evaporation rates (not shown), and ii) moisture advection from the North Atlantic storm track (Dufour et al., 2016; Jakobson & Vihma, 2010). Over the Pacific side of the basin the North Pacific Storm track is found to transport moisture into the Arctic basin (Groves & Francis, 2002; Sorteberg & Walsh, 2008), although the effect hereof is smaller compared to the Atlantic Storm track.

In summer, precipitation is more zonally distributed (Fig. 1d) which is related to: i) a weak, low-pressure system over the Arctic Ocean (observed in both the model output (Linden et al., 2017; Fig. 5d) and reanalyses (Groves & Francis, 2002; Oshima & Yamazaki, 2004)) causes moisture to circulate counter-clockwise over the Arctic, ii) the higher air temperatures result in a more stable near-surface stratification (not shown) and smaller evaporation, and iii) the North Atlantic Storm track is weaker compared to winter (Groves & Francis, 2002), which reduces the precipitation over the North Atlantic. There is also a relatively strong precipitation gradient over land-ocean boundaries (with higher values over land; Fig. 1d) because of increased cyclogenesis over the continents (Serreze & Hurst, 2000). Generally, the total precipitation rate is higher than in winter because the atmosphere can hold more moisture due to higher air temperatures.

The EC-Earth model is generally able to predict the precipitation rates fairly accurately, despite the systematic underestimation in summer (Fig. 1f, predominantly compared to NCEP and NASA). In winter, however, two patterns of error can be distinguished: i) the precipitation to the east of Svalbard is overestimated, and ii) the precipitation to the east of Greenland is underestimated. Both are most likely caused by the difference in sea ice edge between the models since this is in EC-Earth more north-west located than in the reanalyses data (Fig. 1c).

The detrending process resulted in a total precipitation mean with only small fluctuations over time. The bootstrapping of the differences between the EC-Earth model and the reanalysis data hence resulted in significant values for almost every grid point, since even very small absolute differences were significant. The mean values in the control simulation were (except for the regions near the sea ice edge) between that of the lowest and the highest mean value datasets from the reanalysis.

*Precipitation variability*

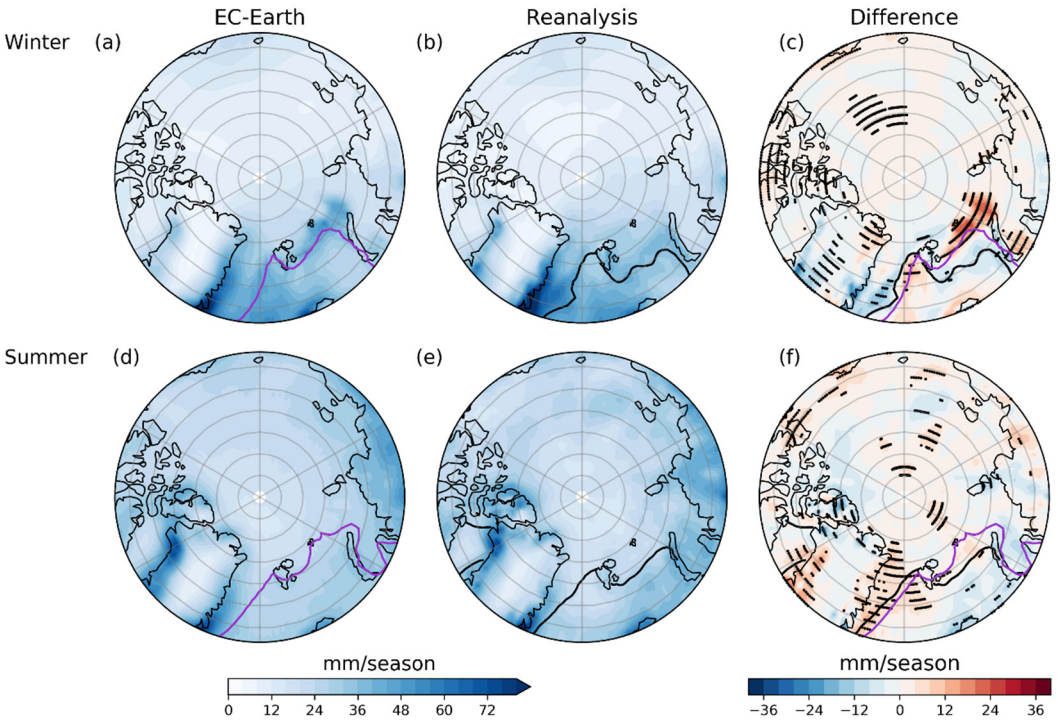


**Figure 2**: Precipitation variability for EC-Earth (the control simulation), reanalyses (defined as the average value for ERA-Interim, NCEP/CSFR, and NASA MERRA-2), and the difference (reanalyses - EC-Earth) for winter (first row) and summer (second row). The purple and black contours indicate the 15% sea ice concentration isopleth. Differences are marked as significant if the 5 and 95 percentiles of the bootstrapped reanalyses and the simulation do not overlap.

The validation of precipitation variability is shown in Fig. 2. During both seasons (Fig. 2a and 2d) the pattern is roughly similar to the mean precipitation (Fig. 1a and 1d, respectively). In winter, precipitation variability is highest over the North Atlantic Ocean (Fig. 2a). This high variability is almost certainly caused by fluctuations in the sea ice border. The passage of cyclones from the North Atlantic storm track and (to a lesser extent) from the Pacific storm track contributes to considerable fluctuations in poleward moisture transport. The east of Greenland exhibits strong variability (Fig. 2a), which in previous studies has been related to the North Atlantic storm track (Groves & Francis, 2002; Sorteberg & Walsh, 2008).

In summer, the precipitation variability is roughly similar to the mean precipitation, i.e. more zonally distributed over the Arctic (Fig. 2d). The magnitude of variability is stronger than that in winter, especially in the central Arctic, because of the relatively higher mean precipitation levels and higher values of moisture in the atmosphere.

For both winter and summer (Fig. 2a, Fig. 2d), the high precipitation variability along the borders of Greenland is related to the large-scale circulation patterns. For example: in positive AO-years during winter, the moisture is transported from the east towards Greenland (Groves & Francis, 2002; their Fig. 15), resulting in precipitation mainly on the eastern side (Suppl. Fig. 1) of the ice sheet due to orographic uplift. In years of negative AO, the same mechanism expectedly happens on the western side of Greenland, as was found by Groves & Francis (2002).

In general, the EC-Earth model slightly overestimated precipitation variability during winter (Fig. 2c), especially over the regions with low variability (an overestimation of 3 mm/season over the Arctic Ocean and Canadian Archipelago). In summer, the differences between the simulation and reanalyses are more spatially scattered (Fig. 2f). The difference in variability between the EC-Earth model and the reanalyses exhibits the same pattern as in mean precipitation, with the largest deviations being related to the difference in sea ice edge location in winter. Otherwise, the regions where the differences are significantly different are comparatively small. We, therefore, conclude that, apart from some local differences, the EC-Earth model is able to accurately simulate precipitation characteristics (means and variability) in the current climate.

### 3.2. Precipitation variability in different climate states

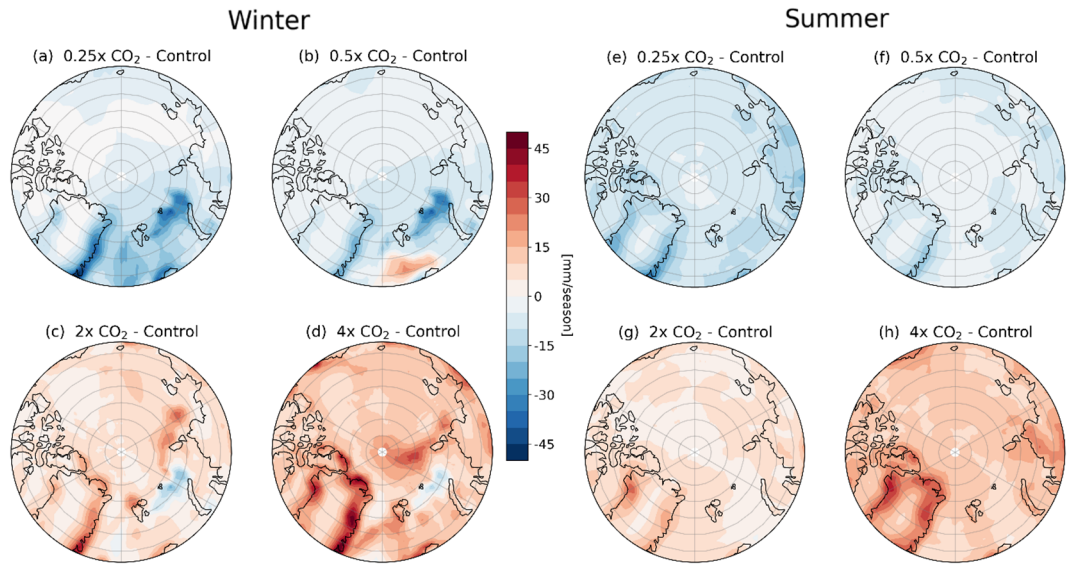


**Figure 3**: Precipitation variability of the four climate states relative to the control climate in winter (left, figures a - d) and summer (right, figures e - h).

The change in precipitation variability between climate states (relative to the control climate) is shown in Fig. 3. Evidently, the total precipitation variability in both seasons increases for climates with higher $CO_2$ concentrations (i.e. warmer climates, the bottom row of Fig. 3). Both seasons exhibit a large increase (decrease) of precipitation variability near the margin of Greenland in warmer (colder) climates.

The increase of precipitation at the Greenland coast is in agreement with recently observed trends (Mernild et al., 2015) and has been attributed to a combination of both atmospheric moisture availability and the passage of cyclones (Schuenemann & Cassano, 2010). The direction from where the moisture is advected determines where the precipitation falls (e.g. on the east- or west coast of Greenland) due to orographic uplift. Because precipitable water increases in warmer climates, more precipitation is forced to fall when the air cools adiabatically as it is pushed upwards by the Greenland Ice Sheet. The opposite happens in colder climates: as less moisture is

available due to colder temperatures and sea ice is extended southwards which reduces moisture uptake from the ocean and unstable situations, less precipitation is formed.

Interestingly, the region north of the Barents Sea exhibits reduced variability for both colder (Fig. 3c and 3d) and warmer climates in winter. This is presumably due to sea ice retreat (which influences the surface evaporation) and enhanced inflow of warm ocean water (which influences the vertical temperature gradient in the lower atmosphere) in warmer climates (Van der Linden et al., 2016; Van der Linden et al., 2019). In colder climates, the opposite situation occurs (Fig. 3a and 3b) as the sea ice expands southwards.

In summer, the variability increase (decrease) towards warmer (colder) climates is more spatially uniform over the ocean, as higher air temperatures reduce the vertical temperature gradients over the ocean, thereby increasing atmospheric stability. The patterns of change in precipitation variability across climate states are quite similar. The magnitude of variability, however, is amplified, especially towards warmer climates. The increase in precipitation variability towards warmer climates is more than twice as large in the 4x $CO_2$ climate (Fig. 3h) than in the 2x $CO_2$ climate (Fig. 3g).

Compared to winter, the changes in summer are more pronounced over the continents. This is in agreement with currently observed trends in which winter oceanic cyclones are more intensified and in summer the increase is more focused over the continents (Tilinina et al., 2013).

To obtain further insight into the mechanisms behind changes in precipitation (means and variability) it is helpful to study the various components of the Arctic's hydrological cycle in the atmosphere. To this end, the mean and variability of the total precipitation, moisture transport across 70 °N, and evaporation are shown in Fig. 4 for both winter and summer for each of the five climate states.

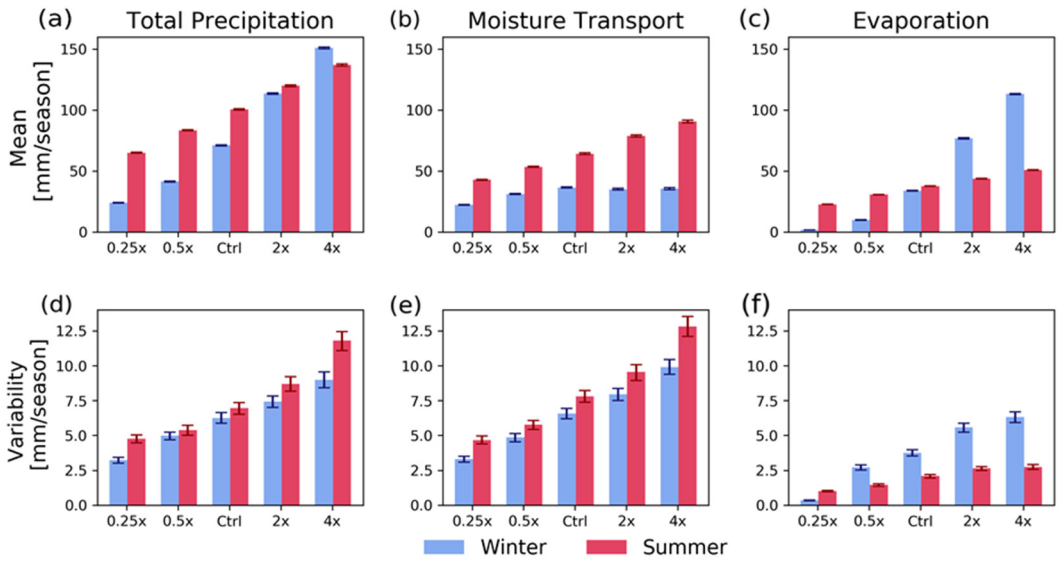


**Figure 4**: The means (top) and variability (bottom) of total precipitation, moisture transport, evaporation in winter (blue) and summer (red) for the five climate states (70 °N – 90 °N). Error bars for variability indicate the 5th and 95th significance percentiles, calculated by bootstrapping the data 1000 times after taking the seasonal average and detrending the data.

*Means*

Total precipitation is lowest in both seasons for the coldest climate and steadily increases towards warmer climates. The total Arctic precipitation is (with the exception of the 4x $CO_2$ climate) lower in winter than in summer.

In winter, the increase in total precipitation is predominately driven by the increase in evaporation (Fig. 4c). Surface evaporation increases in warmer climates because of the retreating sea ice and also the intrusion of relatively warm ocean water into the Arctic, resulting in enhanced energy exchange between the ocean and atmosphere through the latent heat flux.

Poleward moisture transport originates from more southern latitudes, where the atmosphere contains more moisture compared to the Arctic, due to higher ambient temperatures. Due to the Clausius Clapeyron equation, the increase in moisture per degree of warming towards warmer climates is higher in the southward latitudes. However, due to Arctic amplification (which is found

to be the strongest in winter (Screen & Simmonds, 2010; Koenigk et al., 2013) and the related increase in Arctic evaporation, the meridional moisture gradient remains fairly constant towards warmer climates. The differences in the zonal mean of precipitable water (integrated over height) of the various climate states with the control climate are shown in Fig. 5.

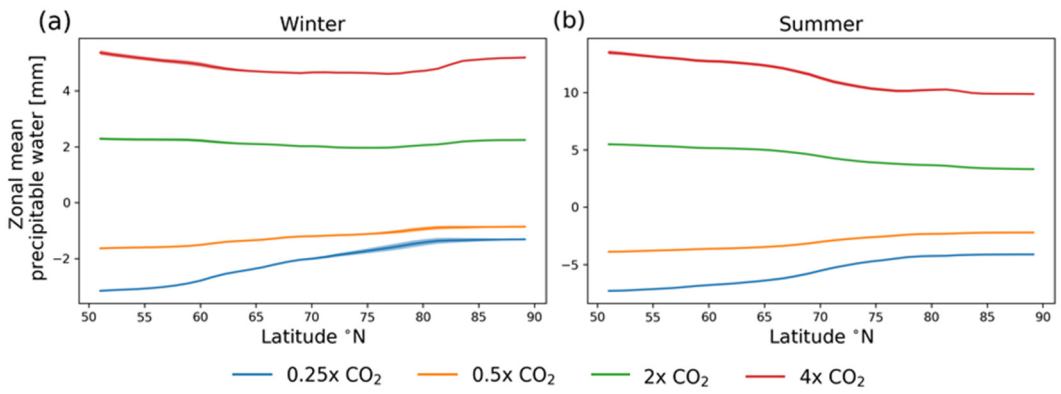


**Figure 5**: Difference in precipitable water between the various climate states and the control climate in (a) winter and (b) summer. The shading indicates the standard deviation (also relative to the control climate).

In summer, the increase in total precipitation is governed by enhanced poleward moisture transport (Fig. 4b). The evaporation only slightly increases (Fig. 4c) because higher air temperatures result in a more stable stratification of the boundary layer over the Arctic Ocean (further elaborated in section 3.5.) The warming-induced increase in vertically integrated precipitable water is amplified in the southern latitudes (Fig. 5b), while at the same time the Arctic amplification is less pronounced in summer (compared to winter). Therefore, the meridional moisture and temperature gradient is increased, which tends to enhance the moisture transport towards the Arctic.

*Variabilities*

For both seasons and for all variables, the Arctic mean precipitation variability increases from cold to warm climates (Fig. 4d). For all climate states, the variability in total precipitation in summer is

(slightly) higher than in winter, whereas the changes in mean precipitation are stronger in winter. Interestingly, the variability of poleward moisture transport increases in winter (Fig. 4e), even though its mean value is relatively constant across the various climates. This suggests that the changes in the variability of the Arctic hydrological cycle do not simply scale with changes in the mean values, implying that other climate mechanisms (such as changes in the large-scale circulation) also contribute to the changes in variability.

The various components of the hydrological cycle in Fig. 4 exhibit three interesting trends that will be evaluated in more detail below: i) the variability in poleward moisture transport in winter increases with warming while the mean is relatively stable, ii) the increase precipitation variability is relatively small compared to the increase in the variability of both evaporation and poleward moisture transport, and iii) the variability in total precipitation is higher in summer than in winter.

### 3.3. Poleward moisture transport in winter

Figure 4b shows that the mean of poleward moisture transport in winter is relatively constant among the various climate states (as discussed in section 3.2), while its variability is increasing towards warmer climates. Even though the poleward moisture transport is fairly constant towards warmer climate states, the level of atmospheric moisture is enhanced.

Figure 5 shows that the precipitable water content increases towards warmer climates (in both the Arctic and the mid-latitudes). The increase in the Arctic is as large as that in the midlatitudes in winter (Fig. 5a) (see section 3.2). This behavior is in contrast to summer, where the increase is more amplified in the southern latitudes than in the northern latitudes (Fig. 5b), thereby increasing the meridional moisture gradient (and resulting enhanced poleward moisture transport, Fig. 4b). Hence, even though the winter poleward moisture transport remains roughly constant (Fig. 4b), the total amount of atmospheric moisture increases. Dufour et al. (2016) also found that the mean poleward moisture transport is not increasing, despite the strong increase in precipitable water, which they attribute to a decreased correlation between wind and precipitable water.

Apart from the availability of moisture, the mean and variability in poleward moisture transport are affected by cyclones (the dynamical component of poleward moisture transport; discussed in more detail in the next sections). Before a cyclone enters the Arctic, it can take up more moisture in warmer climates due to the increased atmospheric moisture content. The corresponding moisture transport will then enhance the precipitable water content in the Arctic.

However, the location of the cyclonic activity is also important: its effect is stronger if cyclones are located in areas with abundantly available moisture. The correlation between poleward moisture transport and sea level pressure is relatively constant across the different climate states during winter, and the North Atlantic storm track is found not to shift northwards in winter. However, the precipitable water content over this area strongly increases. Variability in the North Atlantic storm track is therefore thought to enhance the poleward moisture transport variability due to the abundance of precipitable water in warmer climates.

Hence, while the mean poleward moisture transport is relatively constant due to reinforced Arctic warming (and thus related to the meridional moisture and temperature gradient), the variability is most likely enhanced due to higher atmospheric moisture content and the location of the cyclonic activity (e.g. the North Atlantic storm track is not changing, but the effect of the storm track is increasing due to the abundance of moisture towards warmer climates).

### 3.4. Evaporation and poleward moisture transport during winter

Figure 4 also shows that the variability in both poleward moisture transport and evaporation increases towards warmer climates in winter. The increase towards warmer climates in total precipitation variability is slightly smaller than that in the poleward moisture transport. This is unexpected because: i) there is a strong increase in the mean precipitation, which is expected to influence the variability, and ii) the smaller increase in total precipitation variability compared to the increase of both the poleward moisture transport and the evaporation variability. The smaller magnitude of precipitation variability suggests that poleward moisture transport and evaporation variability are not in phase and have potentially different governing mechanisms.

It is hypothesized that evaporation variability acts primarily on decadal time scales since it is related to the sea surface temperature. Due to the large heat capacity of the ocean, atmosphere-ocean interactions induce low-frequency fluctuations of the surface fluxes (Van der Linden et al., 2016). These variables indeed show correlation (see Tab. 1), and also demonstrate a relatively stronger correlation for decadal variabilities. The low correlation for the 4x $CO_2$ climate is most likely related to the only relatively small area that exhibits decadal variability since the ocean is completely open in this climate.

**Table 1:** Correlations between sea surface temperature and evaporation for the different climate states during winter, evaluated separately for interannual and decadal variabilities. Significant values are marked (* for $p < 0.05$, ** for $p < 0.01$).

| $CO_2$ concentration | Sea Surface Temperature – Evaporation | |
|---|---|---|
| | *Interannual* | *Decadal* |
| 0.25x | 0.54** | 0.42** |
| 0.5x | 0.79** | 0.93** |
| Control | 0.34** | 0.78** |
| 2x | 0.25** | 0.78** |
| 4x | -0.13* | 0.22** |

In contrast, atmospheric moisture transport mechanisms are expected to dominate interannual variability, as atmospheric processes are relatively fast. To assess the time-scale dependence of the processes governing precipitation variability, regressions maps for between the evaporation and the standardized poleward moisture transport are shown in Fig. 6 and 7 for interannual and decadal variability, respectively.

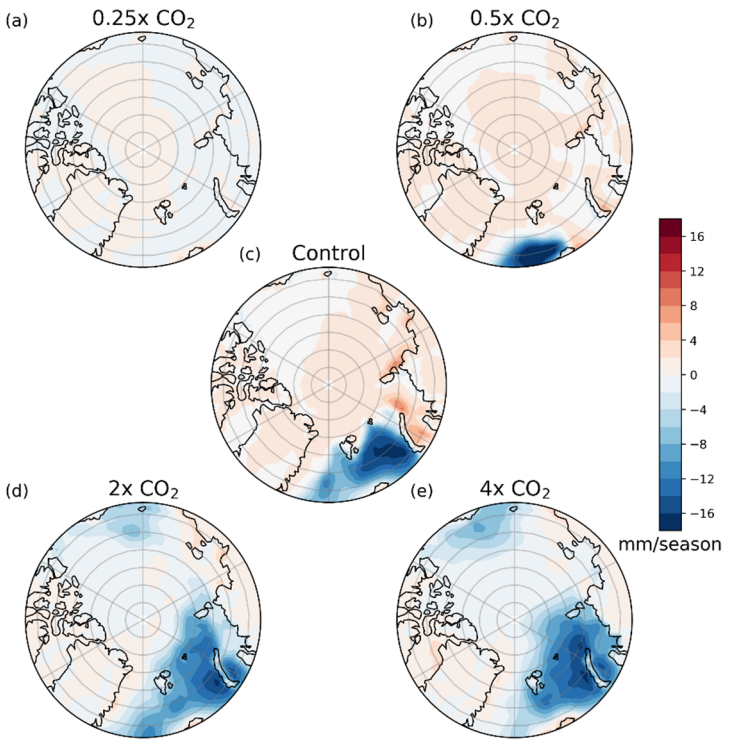


**Figure 6**: Regression maps (70 °N – 90 °N) of surface evaporation on the standardized moisture transport across 70 °N in winter for interannual variabilities. Note that the scaling of Fig. 6 and 7 is different.

In general, negative regressions between winter poleward moisture transport and evaporation depicted in Fig. 6 and 7 can be interpreted as follows. When moist air enters the Arctic, the vertical moisture gradient between the ocean and the atmosphere decreases, which in turn slows down evaporation. On the other hand, if evaporation is enhanced, atmospheric moisture in the Arctic region increases which decreases the meridional moisture gradient, thereby reducing the poleward moisture transport by eddies. Interannual and decadal regressions are discussed separately.

The interannual variability regressions show that the highest values are found over areas where the sea ice permanently retreats (in the 0.5x $CO_2$ climate (Fig. 6b) this happens over the midlatitude North Atlantic, and this region moves north- and eastwards towards warmer climates) and the variability in sea surface temperature is diminished (this also moves further north- and eastwards towards warmer climates).

For Arctic means, surface evaporation and Arctic precipitable water exhibit a negative correlation for interannual variability ($r$ = -0.42 for the 0.25x $CO_2$ climate, $r$ = -0.53 for the control climate and $r$ = -0.73 for the 4x $CO_2$ climate). This indicates that when Arctic precipitable water content is high, evaporation is reduced. In contrast, lower precipitable water values are related to higher evaporation values. Therefore, the interannual variability in precipitable water (and, consequently, evaporation and precipitation) will be mostly determined by the poleward moisture transport. In the three warmest climate states, the regressions slightly reduce over the Atlantic at the southern end of the Arctic basin. This is in agreement with the absolute magnitude of interannual variability in evaporation (not shown), which also exhibits a slight decrease over this area.

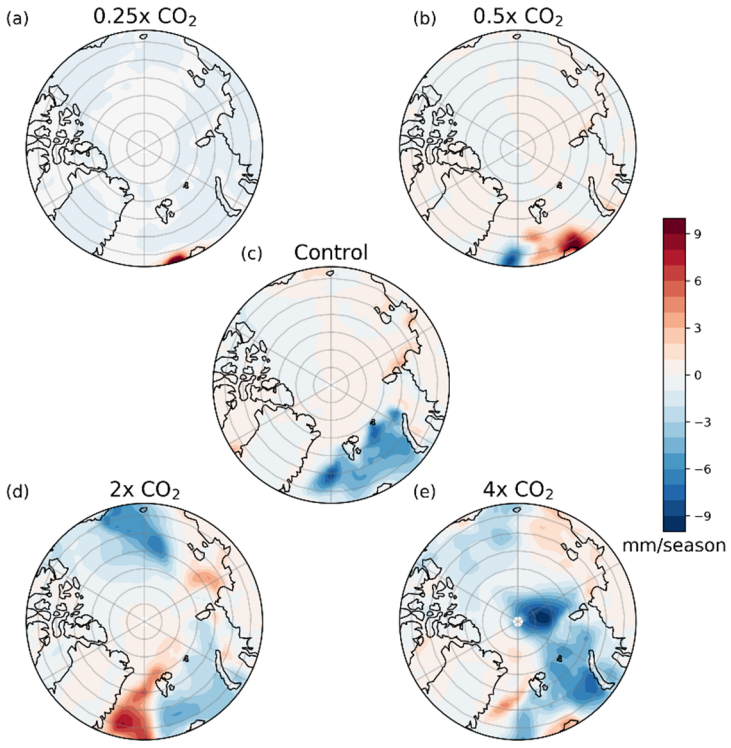


**Figure 7**: Regression maps (70 °N – 90 °N) of surface evaporation on the standardized poleward moisture transport across 70 °N in winter for decadal variabilities. Note that the scaling of Fig. 6 and 7 is different.

The decadal variability (Fig. 7) is, in contrast to the interannual variability, mainly apparent in regions where the sea surface temperature exhibits decadal variability (Suppl. Fig. 2). In the absence of sea ice, warmer ocean water enhances the atmospheric instability over the open oceans in winter. The temperature gradient reinforces turbulent fluxes (increasing evaporation; precipitable water and evaporation exhibit positive correlation values over the areas of decadal sea surface temperature fluctuations), through which the amount of moisture in the atmosphere increases. This higher atmospheric water content opposes poleward moisture transport, resulting in negative regression values between evaporation and poleward atmospheric moisture transport.

For increasingly warm climates, areas of negative regressions expand as more open water is available due to sea ice retreat, both for interannual and decadal variability. Decadal variability between evaporation and poleward moisture transport is primarily located over regions that exhibit fluctuations in sea surface temperature. The variability slightly decreases once the sea ice has disappeared and the decadal variability of the influx of warm ocean water is displaced further northward. As the most prominent sources of oceanic decadal variability diminish towards warmer climates, the poleward atmospheric moisture transport also becomes more important in determining decadal variability over the Atlantic Ocean.

For decadal variability, areas of strongly positive regression values can also be observed in the North Atlantic (e.g. in the 0.5x and 2x $CO_2$ climates). For these regions, increases in evaporation due to sea surface temperature fluctuations result in a positive regression with the poleward moisture transport. In the 2x $CO_2$ climate, strong positive regressions are found close to Greenland (Fig. 7d), which is why we will focus on this area.

Positive regressions between evaporation and poleward moisture transport may be caused by our definition of the moisture transport: a zonal average along the 70 °N latitude circle, meaning that longitudinal variations are ignored. Hence, even if the zonally averaged poleward moisture transport increases, the moisture transport does not necessarily increase along all longitudes.

The discussion of the relation between poleward moisture transport and evaporation focused on the thermodynamic interactions until now. The dynamical components determining the poleward moisture transport (e.g. pressure systems, wind direction) may also play a role. Therefore, the correlation between poleward moisture transport and sea level pressure is evaluated and shown in Fig. 8.

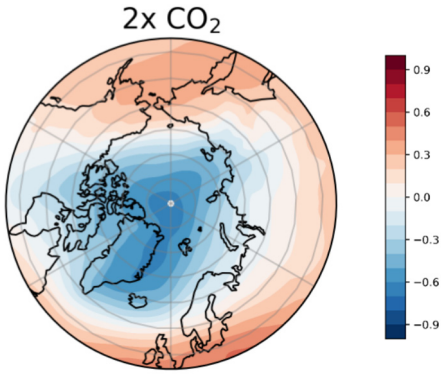


**Figure 8**: Correlation between poleward moisture transport across 70 °N and sea level pressure for the 2x $CO_2$ climate, as this area exhibits strong positive correlation values between atmospheric poleward moisture transport and evaporation.

The region to the east of Greenland (which exhibits positive regression values) is found to exhibit a strong negative correlation between sea level pressure and poleward moisture transport (Fig. 8). This hints at a dynamical component in the differences in the variability of poleward moisture transport between the various climate states. The negative correlation indicates that enhanced poleward moisture transport is associated with lower Arctic surface pressure over this region. Although this was also observed for the control and 4x $CO_2$ climates (not shown), only the 2x $CO_2$ climate exhibited decadal variability in evaporation at this location, which resulted in the positive regression values.

Schuenemann & Cassano (2010) mentioned that increased atmospheric moisture due to enhanced evaporation over the Greenland Sea is transported through cyclones (associated with low-pressure systems) to the east coast of Greenland. Hence, this suggests that evaporation and moisture transport close to the coast of Greenland reinforce each other (especially because the regressions (both interannual and decadal) are never negative across all climate states close to the east coast of Greenland).

When a distinction is made between interannual and decadal variability in atmospheric moisture, evaporation always exhibits a negative correlation for interannual variabilities, while for decadal variabilities it shows positive correlations over regions where the sea surface temperature fluctuates. Therefore, in combination with the results above, it can be concluded that interannual precipitation variability is predominately controlled by poleward moisture transport, whereas decadal variability is predominately controlled by Arctic surface evaporation.

### 3.5. Summer versus winter variability

Figure 4d shows that, going from cold to warm climates, the total precipitation variability increases more in summer than in winter, relatively speaking. In the previous section, we elucidated the role of the interactions between evaporation and poleward moisture transport in winter and hence explained the relatively small increase in wintertime precipitation variability. In summer, the poleward moisture transport and evaporation also exhibit a negative correlation, but the regressions are much weaker (not shown). The lower regression values are expected to be caused by the higher air temperatures due to incoming solar radiation, resulting in a smaller vertical temperature gradient (and therefore moisture gradient) between the ocean and atmosphere (e.g. a more stable stratification of the boundary layer over the Arctic Ocean).

To verify whether stability over the oceans is indeed increased during summer, we analyze the components of the total precipitation (i.e. convective and large-scale) separately. The first is associated with local-scale vertical instabilities (e.g. fluctuations in vertical gradients), while the second is associated with large-scale dynamics (e.g. moisture convergence, orographic uplift).

Therefore, it can be expected that wintertime surface evaporation is positively correlated with convective precipitation, whereas it is negatively correlated with large-scale precipitation (since this is associated with reduced poleward moisture transport, as explained in the previous paragraph). The correlations between convective and large-scale precipitation and with evaporation for both seasons are shown in Table 2.

**Table 2:** Correlations between convective precipitation and large-scale precipitation for the different climate states, evaluated separately for winter and summer. Significant values are marked (* for $p < 0.05$, ** for $p < 0.01$).

| $CO_2$ concentration | Convective – Large-Scale | | Large-Scale – Evaporation | | Convective – Evaporation | |
|---|---|---|---|---|---|---|
| | *Winter* | *Summer* | *Winter* | *Summer* | *Winter* | *Summer* |
| 0.25x | 0.64* | 0.56* | 0.06 | 0.05 | 0.37* | 0.38* |
| 0.5x | 0.48* | 0.53* | 0.14* | -0.23* | 0.76* | 0.10** |
| Control | 0.15* | 0.60* | -0.12** | -0.32* | 0.81* | 0.01 |
| 2x | -0.05 | 0.57* | -0.29* | -0.24* | 0.82* | -0.06 |
| 4x | -0.03 | 0.61* | -0.39* | -0.34* | 0.76* | -0.10 |

The correlation between convective and large-scale precipitation decreases towards warmer climates in winter but remains constant in summer. Table 2 verifies that in winter, except for the coldest climate (in which the ocean is completely frozen), convective precipitation and evaporation exhibit a strong positive correlation, while the correlation between large-scale precipitation and evaporation becomes increasingly negative for warmer climates. This indicates that winters with relatively high large-scale precipitation (due to enhanced poleward moisture transport), the convective precipitation is reduced (as a consequence of the enhanced transport of relatively warm and moist air into the Arctic, the atmospheric instability and evaporation over the oceans are reduced, resulting in less convective precipitation).

In summer, however, both large-scale and convective precipitation are not strongly correlated with evaporation. Due to the ice-free and warmer ocean, convective precipitation is reduced over the

ocean (in agreement with Serreze & Hurst, 2000), and therefore shows a decreasing and even insignificant correlation with evaporation towards warmer climates. Convective precipitation is then more focused over land and is also to a larger degree dependent on the poleward moisture transport. Because large-scale and convective precipitation are both related to poleward moisture transport during summer, both contribute to precipitation variability, thereby increasing its magnitude. This subdivision in precipitation types thus provides an explanation for the differences in precipitation variability changes for summer and winter.

However, it remains unclear why the changes in precipitation variability during summer (with respect to the control climate) are larger than the changes in mean precipitation. The correlation between poleward moisture transport and precipitable water in the Arctic during summer is low across all climate states (not shown). This is due to both the abundance of moisture in summer and less active mechanisms to produce precipitation (like instabilities over the ocean) exist (Groves & Francis, 2002; Serreze & Etringer, 2003).

This low correlation hints at the increased occurrence of more (intense) cyclones in warmer climates in summer. This is supported by several studies (Sorteberg & Walsh, 2008; Tilinina et al., 2013), which found increased activity of summer cyclones over the last 50 years, during which the global (and Arctic) temperature is strongly increasing. To provide an (indirect) indication of the prevalence of cyclones, the correlation between poleward moisture transport and geostrophic wind speeds is shown in Fig. 9 for the three warm climate states in summer.

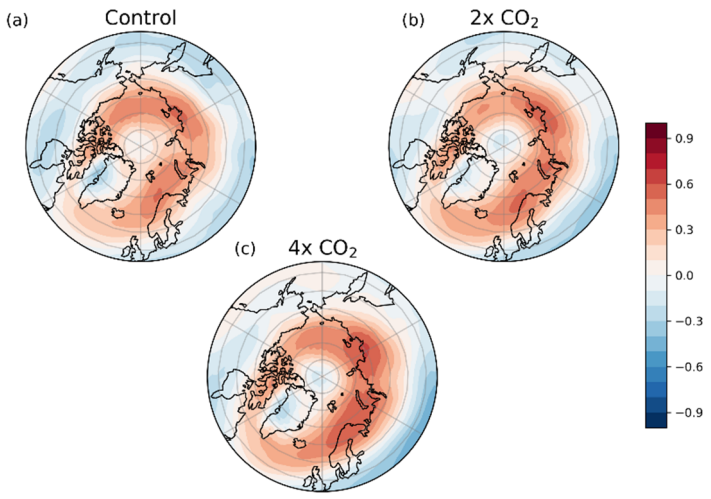


**Figure 9**: Correlation between moisture transport and geostrophic wind-speed at 500 hPa in summer for the three warm climate states.

Figure 9 shows that the correlation between poleward moisture transport and the geostrophic wind speed increases towards warmer climates, especially over northern Eurasia (which is in agreement with recent observations of Tilinina et al., 2013). In this region, the absolute variability of geostrophic wind also increases towards warmer climates (not shown). Hence, in warmer climates, the cyclonic activity is expected to increase, which increases the efficiency (e.g. stronger upward motions) through which precipitation is formed. In combination with the abundance of atmospheric moisture, the increased cyclonic activity leads to enhanced precipitation variability in summer.

Another source of precipitation variability in summer can be attributed to the Arctic Oscillation (AO). To study the influence of AO on Arctic precipitation, regression values of precipitation on the normalized AO-index are shown in Fig. 10 for the various climate states. The correlation is fairly high for all climates and slightly increases towards warmer climates. The regions of highest correlation are located near the Pacific side of the Arctic basin, the Canadian Archipelago, and west Greenland.

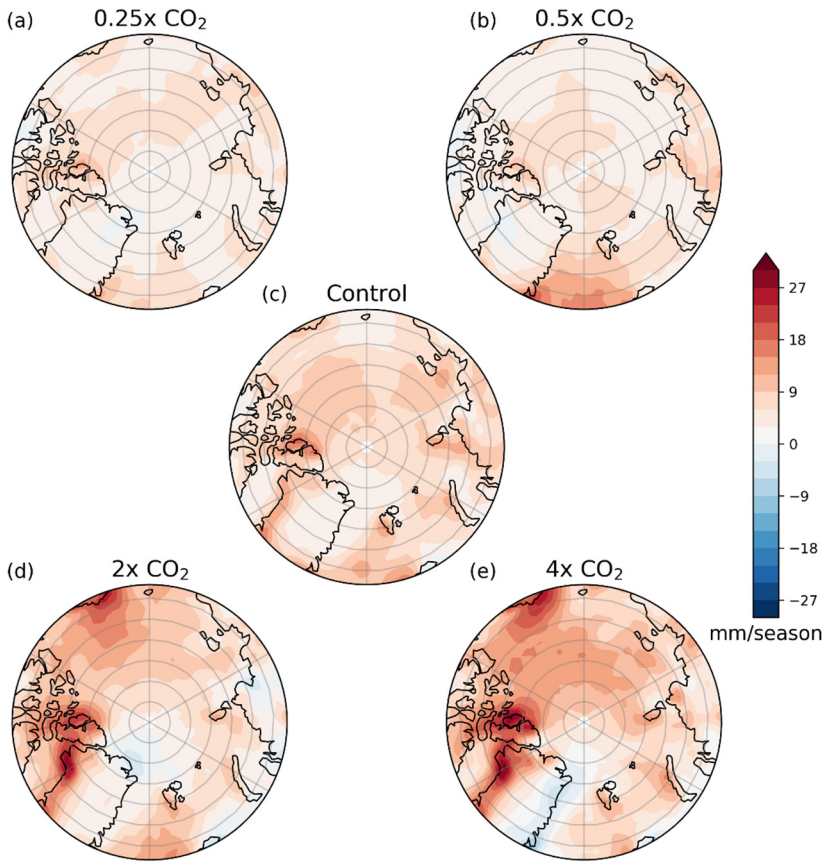


**Figure 10**: Regression of precipitation [mm/season] on the normalized AO-index for the five different climate states. The Arctic average correlation between the AO-index and precipitation variability across different climate states are 0.56, 0.50, 0.61, 0.60, and 0.67, respectively.

Therefore, it can be concluded that Arctic precipitation variability during summer is higher than in winter because of i) more atmospheric moisture, ii) more active cyclonic activity towards warmer climates, and iii) a relatively weak counteracting relation between evaporation and poleward moisture transport due to higher air temperatures in summer.

## 4. Discussion and conclusion

Currently, little is known about the hydrological cycle variability in the Arctic including its dependence on climate. Our study illustrates the effects of changes in the climate on the means and the variability in Arctic precipitation and provides insight into the mechanisms that govern the associated changes in the hydrological cycle across different climate states and time scales. Our results, therefore, help to quantify and interpret changes in climate variability in the Arctic.

The increase in average Arctic precipitation towards warmer climates is attributed mainly to evaporation in the winter (in agreement with Bintanja & Selten (2014) and Dufour et al. (2015) also attribute the observed increase in specific humidity over the past 30 years to evaporation), which is attributed in this study to both sea ice melt and the northward intrusion of warm ocean water. Wintertime precipitation variability is governed by both poleward moisture transport and evaporation, which oppose each other as they both influence the vertical and meridional moisture gradient (e.g. if moisture transport increases, it reduces the vertical moisture gradient, which slows down the evaporation). The poleward moisture transport is found to be dominant on interannual timescales, whereas the evaporation caused by sea surface variability dominates on decadal timescales.

Both the large increase in mean precipitation and the explained conflicting relation between evaporation and poleward moisture transport result in a relatively small change in wintertime precipitation variability towards warmer climate compared to the change in mean precipitation. This is in agreement with the study of Pendergrass et al. (2017). In summer the increase in precipitation variability is larger than the increase in mean towards warmer climates. While in winter the thermodynamic component of moisture transport is found to govern the changes in variability towards warmer climates (and thereby interacting with evaporation), in summer the dynamic component appears to be dominant. Hence, in summer the relatively large increase in summer precipitation variability can be attributed to both i) the relatively small increase in the mean precipitation, and ii) the dominant dynamic component in moisture transport variability. The increase in poleward moisture transport variability in both winter and summer towards warmer

climates is in agreement with observed recent trends in cyclonic activity (Tilinina et al., 2013, Dufour et al., 2016; Sorteberg & Walsh, 2008).

A limitation of this study is that only atmospheric $CO_2$ concentrations were different between the five climates; other components such as land cover (ice, vegetation) and other gas concentrations were held at their current levels/distributions. While this is not a realistic scenario for the future climate, this study aims at understanding the processes associated with Arctic variability and its dependence on climate, rather than quantifying such changes in a realistic future scenario (as done by Bintanja et al., *under review*).

Only one global climate model (EC-Earth) was used here because it is the only model that we know of for which long (time period larger than 500 years) equilibrium climates other than the current climate were simulated. We validated the simulated variability in Arctic precipitation with reanalyses data and found largely similar values for the current climate. A recent multi-model (CMIP5) study supports our results, i.e. the increasing importance of evaporation for mean precipitation, and the importance of the poleward moisture transport in explaining projected increases in Arctic interannual precipitation variability towards warmer climates (Bintanja et al., *under review*).

For practical reasons, monthly data was used in this study. This timescale makes it more difficult to link variabilities to the cyclonic activity because those mostly have a time scale of shorter than a month. Also, this makes it unfeasible to perform a lead-lag analysis between evaporation within the Arctic and moisture transport across 70 °N, because the transport of moisture from the extra-tropics towards the Arctic also has a shorter timeframe.

The time series were filtered with a Butterworth filter with a cut-off frequency of 0.1 $yr^{-1}$ to distinguish between interannual and decadal variabilities. We also explored the use of a rolling window to smooth the signals, but the Butterworth filter was found to possess a sharper cut-off (Suppl. Fig. 3).

Although the magnitude of geostrophic wind at 500 hPa is considered to be a good indicator for the location of the storm tracks (Wallace et al., 1988), it is difficult to separate the changes in moisture transport due to either the thermodynamical ($q$) or the dynamical ($v$) component. Inclusion of the wind component would enable differentiation between the mean, time deviation, and zonal deviations of the moisture transport (Boer et al., 2001; Dufour et al., 2016) and hence might provide new insights in the origin of precipitation variability.

A better understanding of variability is important because long-term variability can obscure trends and is associated with precipitation extremes (Pendergrass et al., 2017). Increased variability modifies the run-off, which can alter changes in the salinity distribution of the ocean and thereby the oceanic circulation (Davies et al., 2014). On top of that, the changes in variability are especially enhanced in regions with amplified mean changes, e.g. the margins of Greenland, increasing the possibility of reaching a tipping point with irreversible consequences (Rahmstorf, 1995).

This study showed that precipitation variability increases towards warmer climates and does not directly scale with an increasing mean. To our knowledge, this is the first study discussing both the interannual and decadal variability in precipitation, in which also a seasonal distinction is made. Because the mechanisms behind variability are found to be seasonal and climate state dependent, this study contributed a better understanding of the Arctic hydrological cycle variability.

## References


Bengtsson, L., Hodges, K. I., Koumoutsaris, S., Zahn, M., & Keenlyside, N. (2011). The changing atmospheric water cycle in Polar Regions in a warmer climate. Tellus, Series A: Dynamic Meteorology and Oceanography, 63(5), 907–920.

Bintanja, R., & Selten, F. M. (2014). Future increases in Arctic precipitation linked to local evaporation and sea-ice retreat. Nature, 509(7501), 479–482.

Bintanja, R., Van der Wiel, K., Van der Linden, E.C., Reussen, J., Bogerd, L., Krikken, F. & Selten, F. M. Strong future increase in Arctic precipitation variability linked to poleward moisture transport. Science Advances. *Under review.*

Boer, G. J., Fourest, S., & Yu, B. (2001). The signature of the Annular Modes in the moisture budget. Journal of Climate, 14(17), 3655-3665.

Davies, F. J., Renssen, H., & Goosse, H. (2014). The Arctic freshwater cycle during a naturally and an anthropogenically induced warm climate. Climate Dynamics, 42(7–8), 2099–2112.

Dee, D. P., Uppala, S. M., Simmons, A. J., Berrisford, P., Poli, P., Kobayashi, S., et al. (2011). The ERA-Interim reanalysis: Configuration and performance of the data assimilation system. Quarterly Journal of the Royal Meteorological Society, 137(656), 553–597.

Deser, C., Walsh, J. E., & Timlin, M. S. (2000). Arctic sea ice variability in the context of recent atmospheric circulation trends. Journal of Climate, 13(3), 617–633.

Dufour, A., Zolina, O., & Gulev, S. K. (2016). Atmospheric moisture transport to the arctic: Assessment of reanalyses and analysis of transport components. Journal of Climate, 29(14), 5061–5081.

Eastman, R., & Warren, S. G. (2010). Interannual variations of arctic cloud types in relation to sea ice. Journal of Climate, 23(15), 4216–4232

Gelaro, R., McCarty, W., Suárez, M. J., Todling, R., Molod, A., Takacs, L., et al. (2017). The modern-era retrospective analysis for research and applications, version 2 (MERRA-2). Journal of Climate, 30(14), 5419–5454.

Gillett, N. P. (2002). How linear is the Arctic Oscillation response to greenhouse gases? Journal of Geophysical Research, 107(D3).

Groves, D. G., & Francis, J. A. (2002). Variability of the Arctic atmospheric moisture budget from TOVS satellite data. Journal of Geophysical Research Atmospheres, 107(24).

Hassol, S. J. (2006). Arctic Climate Impact Assessment. Avoiding dangerous climate change, 205.

Hawkins, E., & Sutton, R. (2009). The Potential to Narrow Uncertainty in Regional Climate Predictions. Bulletin of the American Meteorological Society, 90(8), 1095–1108.

Held, I. M., & Soden, B. J. (2006). Robust Responses of the Hydrological Cycle to Global Warming. Journal of Climate, 19(21), 5686–5699.

IPCC. (2013). Intergovernmental Panel on Climate Change Working Group I. Climate Change 2013: The Physical Science Basis. Long-term Climate Change: Projections, Commitments and Irreversibility. Cambridge University Press, New York, 1029–1136.

Jakobson, E., & Vihma, T. (2010). Atmospheric moisture budget in the Arctic based on the ERA-40 reanalysis. International Journal of Climatology, 30(14), 2175–2194.

Koenigk, T., Brodeau, L., Graversen, R. G., Karlsson, J., Svensson, G., Tjernström, M., et al. (2013). Arctic climate change in 21st century CMIP5 simulations with EC-Earth. Climate Dynamics, 40(11–12), 2719–2743.

van der Linden, E. C., Bintanja, R., Hazeleger, W., & Graversen, R. G. (2016). Low-frequency variability of surface air temperature over the Barents Sea: causes and mechanisms. Climate dynamics, 47(3-4), 1247-1262.

van der Linden, E. C., Bintanja, R., & Hazeleger, W. (2017). Arctic decadal variability in a warming world. Journal of Geophysical Research, 122(11), 5677–5696.

van der Linden, E. C., Le Bars, D., Bintanja, R., & Hazeleger, W. (2019). Oceanic heat transport into the Arctic under high and low $CO_2$ forcing. Climate Dynamics, *In press*

Meehl, G. A., Gent, P. R., Arblaster, J. M., Otto-Bliesner, B. L., Brady, E. C., & Craig, A. (2001). Factors that affect the amplitude of El Nino in global coupled climate models. Climate Dynamics, 17(7), 515–526.

Meier, W. N., Gerland, S., Granskog, M. A., Key, J. R., Haas, C., Hovelsrud, G. K., et al. (2012). Arctic Climate Issues 2011: Changes in Arctic Snow, Water, Ice and Permafrost.

Mernild, S. H., Hanna, E., Mcconnell, J. R., Sigl, M., Beckerman, A. P., Yde, J. C., et al. (2015). Greenland precipitation trends in a long-term instrumental climate context (1890-2012): Evaluation of coastal and ice core records. International Journal of Climatology, 35(2), 303–320.

Oshima, K., & Yamazaki, K. (2004). Seasonal variation of moisture transport in polar regions and the relation with annular modes*. Polar Meteorol. Glaciol, 18, 30-53.

Pendergrass, A. G., Knutti, R., Lehner, F., Deser, C., & Sanderson, B. M. (2017). Precipitation variability increases in a warmer climate. Scientific Reports, 7(1), 1–9.

Pinto, J. G., Ulbrich, U., Leckebusch, G. C., Spangehl, T., Reyers, M., & Zacharias, S. (2007). Changes in storm track and cyclone activity in three SRES ensemble experiments with the ECHAM5/MPI-OM1 GCM. Climate Dynamics, 29(2–3), 195–210.

Rahmstorf, S. (1995). Bifurcations of the Atlantic thermohaline circulation in response to changes in the hydrological cycle. Nature, 378(6553), 145.

Reussen, J., Van der Linden, E.C., Bintanja, R. Differences between Arctic interannual and decadal variability across climate states. *Under review.*

Rind, D., Perlwitz, J., & Lonergan, P. (2005). AO/NAO response to climate change: 1. Respective influences of stratospheric and tropospheric climate changes. Journal of Geophysical Research D: Atmospheres, 110(12), 1–15.

Saha, S., Moorthi, S., Pan, H.-L., Wu, X., Wang, J., Nadiga, S., et al. (2010). The NCEP Climate Forecast System Reanalysis. Bulletin of the American Meteorological Society, 91(8), 1015–1058.

Schuenemann, K. C., & Cassano, J. J. (2010). Changes in synoptic weather patterns and Greenland precipitation in the 20th and 21st centuries: 2. Analysis of 21st century atmospheric changes using self-organizing maps. Journal of Geophysical Research Atmospheres, 115(D5), 1–18.

Screen, J. A., Deser, C., Simmonds, I., & Tomas, R. (2014). Atmospheric impacts of Arctic sea-ice loss, 1979-2009: Separating forced change from atmospheric internal variability. Climate Dynamics, 43(1–2), 333–344.

Screen, J. A., & Simmonds, I. (2010). The central role of diminishing sea ice in recent Arctic temperature amplification. Nature, 464(7293), 1334.

Serreze, M. C., & Etringer, A. J. (2003). Precipitation characteristics of the Eurasian Arctic drainage system. International Journal of Climatology, 23(11), 1267–1291.

Serreze, M. C., & Francis, J. A. (2006). The Arctic amplification debate. Climatic change, 76(3-4), 241-264.

Serreze, M. C., & Hurst, C. M. (2000). Representation of mean arctic precipitation from NCEP-NCAR and ERA reanalyses. Journal of Climate, 13(1), 198-201.

Sorteberg, A., & Walsh, J. E. (2008). Seasonal cyclone variability at 70°N and its impact on moisture transport into the Arctic. Tellus, Series A: Dynamic Meteorology and Oceanography, 60 A(3), 570–586.

Taylor, K. E., Stouffer, R. J., & Meehl, G. A. (2012). An overview of CMIP5 and the experiment design. Bulletin of the American Meteorological Society, 93(4), 485–498.

Thompson, D. W. J., & Wallace, J. M. (1998). The Arctic oscillation signature in the wintertime geopotential height and temperature fields. Geophysical Research Letters, 25(9), 1297–1300.

Tilinina, N., Gulev, S. K., Rudeva, I., & Koltermann, P. (2013). Comparing cyclone life cycle characteristics and their interannual variability in different reanalyses. Journal of Climate, 26(17), 6419–6438.

Valcke, S., Caubel, A., Declat, D., & Terray, L. (2003). OASIS3 ocean atmosphere sea ice soil user's guide. Prisim Project Report, (2).

Vavrus, S., & Harrison, S. P. (2003). The impact of sea-ice dynamics on the Arctic climate system. Climate Dynamics, 20(7–8), 741–757.

Wallace, J. M., Lim, G. H., & Blackmon, M. L. (1988). Relationship between cyclone tracks, anticyclone tracks and baroclinic waveguides. Journal of the atmospheric sciences, 45(3), 439-462.

Zhang, J., Lindsay, R., Schweiger, A., & Steele, M. (2013). The impact of an intense summer cyclone on 2012 Arctic sea ice retreat. Geophysical Research Letters, 40(4), 720–726.

## Supplemental material

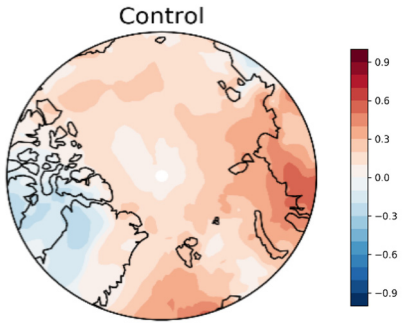


**Figure 1**: Correlation between total precipitation and the AO-index during winter for the control climate.

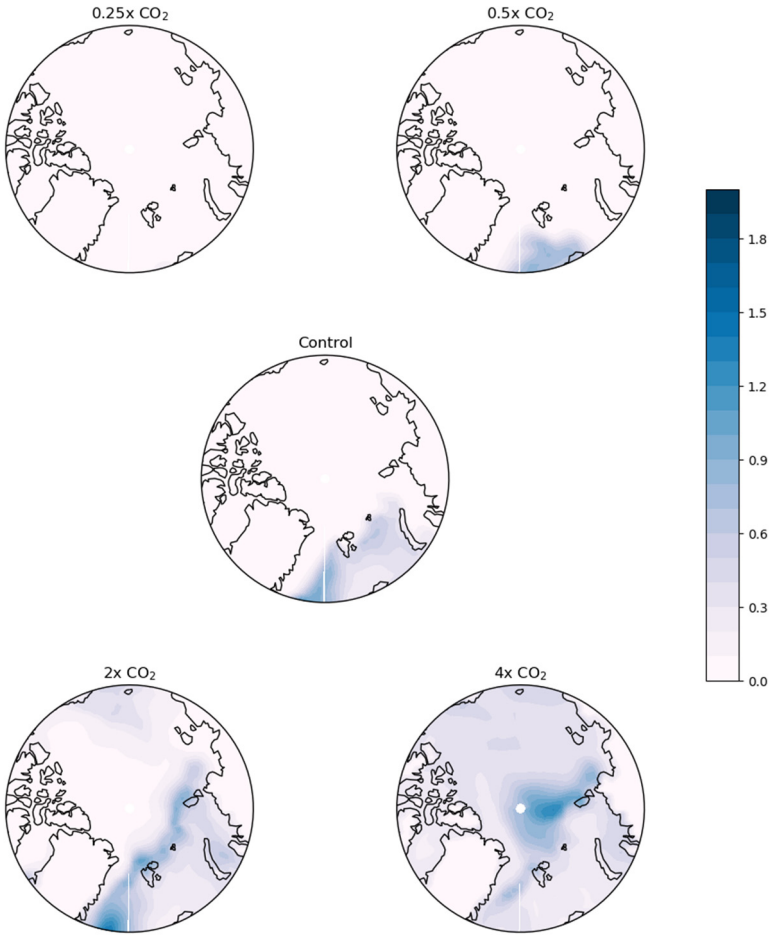


**Figure 2**: Decadal variability in sea surface temperature [K] across different climate states.

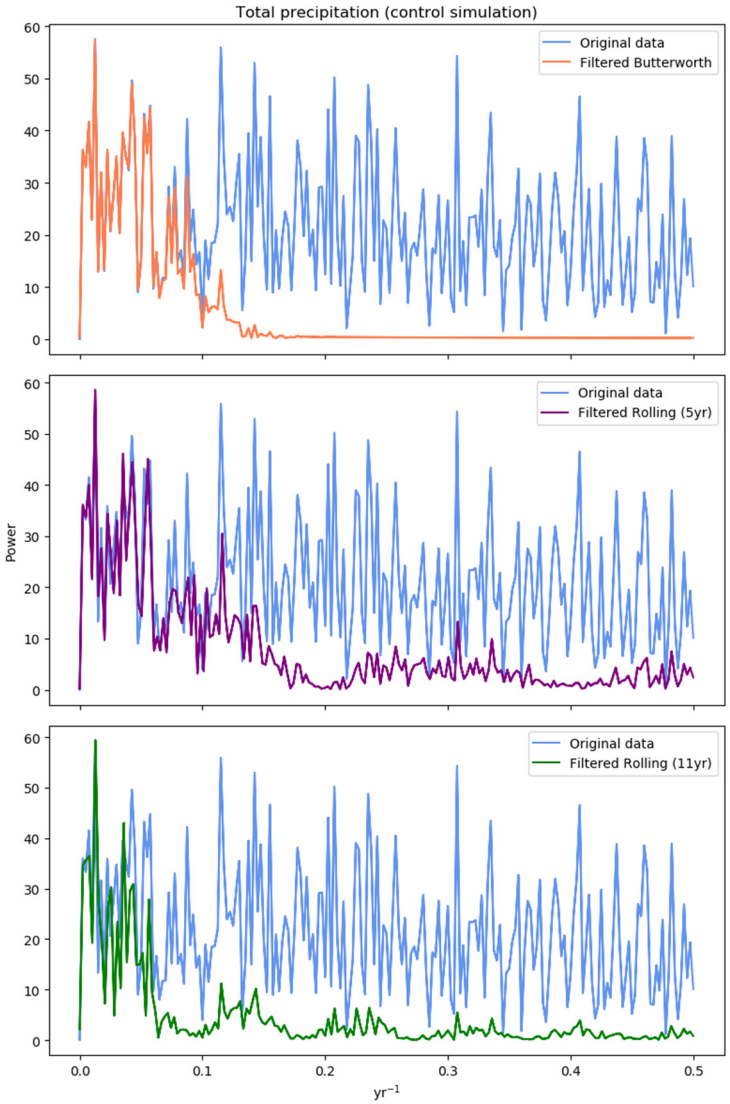


**Figure 3**: Comparison between the performance of the Butterworth filter (top) and rolling window method (middle and bottom).